

Kinetics of Oxide Formation on Carbon Steel Surface in the Presence of Oxygen-Nitrogen Mixtures

Sarita Weerakul^a, Frank R. Steward^{*b}, Thirasak Rirkksomboon^{ac}, Andrew Feicht^b, Chutima Kongvarhodom^b

^aThe Petroleum and Petrochemical College, Chulalongkorn University, Bangkok, Thailand

^bCentre for Nuclear Energy Research, University of New Brunswick, Fredericton, NB, Canada

^cCenter of Excellence on Petrochemical and Materials Technology, Bangkok, Thailand

fsteward@unb.ca

The formation of oxides at 400 °C and 90 °C with two different oxygen concentration conditions on carbon steel surface was studied. From 400 °C tests, oxide films were observed in both conditions. The oxide formed on the surfaces which were exposed to an atmosphere with no change in O₂ concentration was Hematite. On the surfaces which were exposed to an atmosphere with change in O₂ concentration, Magnetite and Hematite were found due to the different exposure time and different conditions of the apparatus. The thickness of the oxide film formed on each membrane was calculated from the weight gained by the membrane and the kinetics of oxide formation on each condition was modelled. From the 400 °C exposure, the reaction rate was controlled by diffusion of O₂ through the oxide layer. The diffusivity of oxygen through the oxide layer, D_{O_2} , was calculated from the rate of oxide formed on the surfaces which were exposed to an atmosphere with no change in O₂ concentration and was found to be $D_{O_2} = 7.055 \times 10^{-14} \text{ m}^2/\text{s}$ and the parabolic rate constant, $k_p = 1.089 \times 10^{-17} \text{ m}^2/\text{s}$. D_{O_2} was used in the prediction of oxide form in the atmosphere with changing O₂ concentration. From the 90°C exposure, weight gains on the membranes were not significant and no oxide films were observed.

1. Introduction

A Hydrogen Effusion Probe (HEP) is a device which monitors the wall thinning from Flow Accelerated Corrosion (FAC) in industrial pipes by measuring the quantity of hydrogen effused through the pipe wall. The atomic hydrogen, produced by the corrosion at the pipe inner surface, effuses through the pipe wall and forms molecular hydrogen at the outside surface. The rate of hydrogen effusing through the pipe walls can be related to the rate of metal loss by corrosion. This relation can be used to calculate the wall thinning rate. The Centre for Nuclear Energy Research (CNER) has developed a HEP instrument which has an initial purpose for measuring the rate of corrosion on the inside of nuclear reactor feeder pipes. However, this instrument can also be used in other industries for example, the petroleum and petrochemical industry and other chemical industries. An important aspect of the HEP is how fast that hydrogen can effuse through the pipe wall to give an online measurement.

Previous fundamental studies of the principles and transport of hydrogen through a carbon steel pipe from FAC have been carried out at CNER (Leelasangjai 2009). These studies identified the effect of air (oxygen) within the instrument installed on the vessel (or pipe) surface which reduces the effusion of hydrogen into the measuring device. Many previous studies (Piggott and Siarkowski 1972; Pyun and Oriani 1989; Bruzzoni, Carranza et al. 1999) show that the iron oxide films on a steel surface will act as a barrier for hydrogen diffusion. Schomberg and Grabke (1996) suggested that iron oxide films will

inhibit the adsorption of hydrogen on the metal surface which inhibits the dissociation to atomic hydrogen required for diffusion through the metal wall. Most studies have been on the effect of at the entrance phase but significantly less for the exit phase.

The purpose of this research is to determine the effect of oxide type and thickness on the exit side on the diffusion of hydrogen through carbon steel membranes. It includes a determination of the type of oxide that will form on the membranes and characteristics of these oxide films. The rate of oxide formation on the vessel surface was determined from the weight gain on the membranes, and a direct measurement from SEM after the experiment is complete.

2. Experimental

A material used for CANDU reactor feeder pipes, carbon steel ASTM A-106B, was selected for these test. According to the constructed test section installed at the Point Lepreau Generating Station (PLGS), it has been calculated that the internal volume is $1.3 \times 10^{-5} \text{ m}^3$ and the exposed surface area of the membrane to the internal volume is $3.5 \times 10^{-4} \text{ m}^2$. For an average plant installation a footprint of $2.0 \times 10^{-3} \text{ m}^2$ and an internal volume of $1.0 \times 10^{-5} \text{ m}^3$ is expected, thus a ratio of $2.0 \times 10^2 \text{ m}^2/\text{m}^3$. Therefore, of $2.3 \times 10^{-3} \text{ m}^2$ extra polished surface was required for each experiment.

2.1 Apparatus

The apparatus is shown in Figure 1. The flanges and membrane were placed in the furnace and connected to a pressure transducer installed outside the furnace. The flanges and tubing were oxidized at 400 °C for 14 days before use in order to prevent oxidation on the flanges and tubing surfaces during the experiment. The pressure transducer and a thermocouple were connected to a data acquisition system and a computer. The membrane was installed between two flanges; one side connected to the pressure transducer to measure the pressure change with time. This side of the membrane will be exposed to the atmosphere with changing O₂ concentration (A-side). The other side is exposed to the atmosphere with no change in O₂ concentration (B-side). Both sides of the membrane were analysed.

2.2 Surface preparation

Surface preparation of each sample was required in order to eliminate any oxide film that may be present and provide a consistent starting surface condition. Each sample was polished with abrasive papers; 60, 120, 240, 400, 600, 800 and 1200 grit, then further polished with diamond solution (6 µm and 1 µm) on nylon cloth. After polishing in each step the surface was rinsed using acetone and dried by lint free tissue. All samples were stored in an argon-purged desiccator while waiting for the test.

2.3 Test procedure

The sample which included a membrane and a wire (extra surface) were installed in the test section. The furnace was turned on in order to raise the temperature to the desired value. The exposure time was started when the temperature reached the test temperature. The furnace was turned off after the exposure time (in Table 1) was reached and allowed to cool over night. The samples were removed and kept in the argon-purged desiccator to await surface analysis.

Table 1: Test Matrix

	Run	Temperature	Exposure time
Set 1	1	400 °C	14 d
	2		7 d
	3		1 d
	4	90 °C	14 d
	5		7 d
	6		1 d
Set 2	7	400 °C	7 d
	8		1 d
	9		5 h

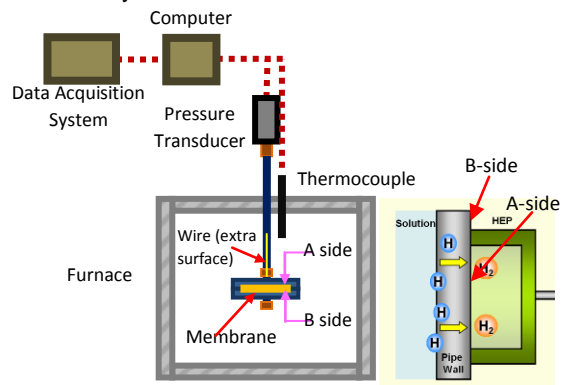


Figure 1: Apparatus with one membrane assembly and schematic of the HEP cup.

3. Results and discussion

3.1 Surface analysis

SEM images show the carbon steel surfaces after the 400°C exposure (Figure 2). On the B-side (exposed to the environment with no change in O₂ concentration during the exposure), the form of oxide is micaceous, but with a different size due to the exposure time; the longer the exposure time, the bigger the sizes of the flakes. From the Raman spectra (Figure 3a), these oxides are Hematite (Fe₂O₃). The experiment for A-side (exposed to the environment with change in O₂ concentration during the exposure), was divided into 2 sets. In the first set of experiments, for the 1 and 7 day exposure, the form of oxide is mainly micaceous (Figure 2: 1A-1 and 7A-1). Raman spectra (Figure 3b) show the oxides are mainly Hematite (Fe₂O₃). The oxide form for 14 day exposure (Figure 2: 14A-1) is granular Magnetite (Fe₃O₄). The second set of experiments was performed in order to confirm that Magnetite formed on the A-side. Magnetite was found on 7 days and 1 day exposures, however, on 5 hours exposure some Hematite was found. From Raman spectra, the mixture of Magnetite and Hematite was found on some parts of the surface (Figure 3c: 5hrA-2) and the characteristic peak of Hematite was a weak peak, which means the area is mainly Magnetite.

For the 90°C exposure, colour change and oxide was not observed. The surface images and the Raman spectra for both sides of the membrane was the same as fresh polished membrane.

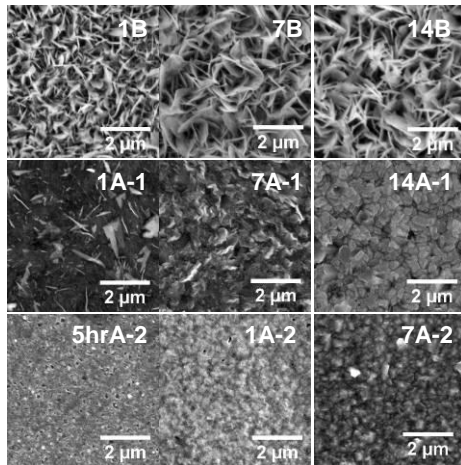


Figure 2: SEM images of carbon steel surfaces exposed to 400 °C.

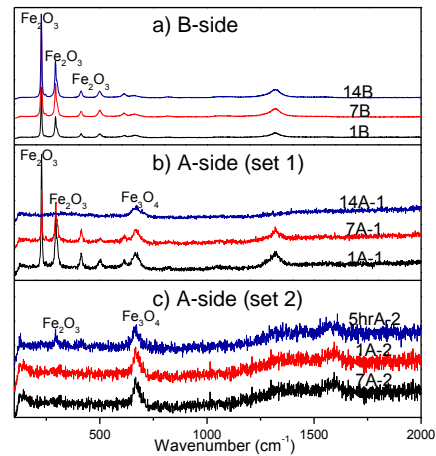


Figure 3: Raman spectra of carbon steel surfaces exposed to 400 °C.

Equilibrium of the transformation of Magnetite to Hematite using thermodynamic data was determined to predict the oxide type that will form on the carbon steel surfaces at 400 °C. The reaction is written as



The partial pressure of oxygen at equilibrium, P_{O_2} , was determined from the following equations;

$$\ln K_p = -\frac{\Delta G_{298}}{RT_0} + \frac{\Delta H_0}{R} \left(\frac{1}{T_0} - \frac{1}{T} \right) + \frac{a_i}{R} \ln \frac{T}{T_0} + \frac{b_i}{2R} (T - T_0) + \frac{c_i}{6R} (T^2 - T_0^2) + \frac{d_i}{2R} \left(\frac{1}{T^2} - \frac{1}{T_0^2} \right) \quad (2)$$

$$\Delta H_0 = \Delta H_{298} - a_i T_0 - \frac{b_i T_0^2}{2} - \frac{c_i T_0^3}{3} + \frac{d_i}{T_0^2}, C_{p_i} = a_i + b_i T + \frac{d_i}{T^2} \text{ and } K_p = \frac{1}{P_{O_2}} \quad (3)$$

where P_{O_2} = partial pressure of oxygen at equilibrium (atm), K_p = equilibrium constant, T = temperature (K), $T_0 = 298$ K, ΔG_{298} = standard free energy = -105,400 cal/mol, ΔH_{298} = standard enthalpy = -123,400

cal/mol , R = ideal gas constant = $1.9858775 cal/mol\cdot K$, and $a_i = -24.83 cal/mol\cdot K$, $b_i = 0.0207 cal/mol\cdot K^2$, $c_i = 0 cal/mol\cdot K^3$, and $d_i = 1.637\times 10^6 cal\cdot K^2/mol$.

At $400^\circ C$, the reaction thermodynamically predicts Hematite even if at a very low oxygen pressure ($4.45526\times 10^{-25} atm$). However, Magnetite formed on the carbon steel surfaces exposed to the environment which changes in oxygen concentration during the exposure. Therefore, kinetics must be significant with respect to the form of oxide produced.

3.2 Kinetics of oxide formation at $400^\circ C$ in an atmosphere with no change in O_2 concentration

From the previous surface information, at exposure the oxide formed on the B-side (exposed to an atmospheric with no change in O_2 concentration) is Hematite (Fe_2O_3). The reaction is as follows:



There are two possibilities that govern the rate of oxide formation; the diffusion of oxygen through oxide layer and the reaction rate. The relations of oxide layer thickness and exposure time which is governed by the diffusivity of oxygen through oxide layer can be derived, which yields;

$$\frac{dx}{dt} = \frac{4 C_{O_2} D_{O_2} MW_{Fe_2O_3}}{6 x \rho_{Fe_2O_3}} \text{ or } x^2 = \frac{4 C_{O_2} D_{O_2} MW_{Fe_2O_3} t}{3 \rho_{Fe_2O_3}} \quad (5)$$

and the relations of oxide layer thickness and exposure time which is governed by the rate of reaction;

$$\frac{dx}{dt} = \frac{4 r C_{O_2} m_{Fe} MW_{Fe_2O_3}}{6 MW_{Fe} \rho_{Fe_2O_3}} \text{ or } x = \frac{4 r C_{O_2} m_{Fe} MW_{Fe_2O_3} t}{6 MW_{Fe} \rho_{Fe_2O_3}} \quad (6)$$

Where D_{O_2} = the diffusivity of oxygen through an oxide layer (m^2/s), C_{O_2} = the concentration of oxygen in surroundings (mol/m^3), $MW_{Fe_2O_3}$ = the molecular weight of Fe_2O_3 (g/mol), MW_{Fe} = the molecular weight of Fe (g/mol), m_{Fe} = the mass of Fe reacted (g), $\rho_{Fe_2O_3}$ = the density of Fe_2O_3 (g/m^3), x = the oxide layer thickness (m), and t = time (s).

The relation between the oxide thickness and time (Figure 4) shows that the rate of oxide formation on carbon steel A106B at $400^\circ C$ in an atmosphere with no change in O_2 concentration (B-side) can be explained by diffusion of oxygen through the oxide layer. From Linear fit of x^2 and based on Hematite formed, D_{O_2} was determined. From Eq. 5, and the parabolic rate; $x^2 = k_p t + c$, Thus

$$slope = k_p = \frac{4 C_{O_2} D_{O_2} MW_{Fe_2O_3}}{3 \rho_{Fe_2O_3}} \quad (7)$$

The slope of the Linear fit is $0.94076 \mu m^2/day$ or $1.089\times 10^{-17} m^2/s$. Therefore, the parabolic rate constant, k_p is $1.089\times 10^{-17} m^2/s$, and D_{O_2} is $7.05545\times 10^{-14} m^2/s$. This diffusivity was further used in the determination of kinetics of oxide formation in an atmosphere with change in O_2 concentration.

3.3 Kinetics of oxide formation at $400^\circ C$ in an atmosphere with change in O_2 concentration

In experimental set 1 (A-side-1), assuming all oxides formed are Fe_2O_3 , the concentration of oxygen inside the cavity based on oxygen reacted to form the boundary layer is

$$C_{O_2}(x) = C_{O_2,0} - \frac{3 \rho_{Fe_2O_3} Ax}{2 MW_{Fe_2O_3} V_C} \quad (8)$$

Applying Eq. 8 into Eq. 5, yields

$$\frac{x}{\left(1 - \frac{3 \rho_{Fe_2O_3} Ax}{2 MW_{Fe_2O_3} V_C C_{O_2,0}}\right)} dx = \frac{2 D_{O_2} MW_{Fe_2O_3} C_{O_2,0}}{3 \rho_{Fe_2O_3}} dt \quad (9)$$

Integrating Eq. 9 becomes

$$x - \frac{b}{a} \ln(ax + b) = act; \text{ where } a = -\frac{3 \rho_{Fe_2O_3} A}{2 MW_{Fe_2O_3} V_C C_{O_2,0}}, b = +1.0, \text{ and } c = \frac{2 D_{O_2} MW_{Fe_2O_3} C_{O_2,0}}{3 \rho_{Fe_2O_3}} \quad (10)$$

Using data in Table 2, the plot of oxide layer thickness (x) versus exposure time (t) from Eq. 10 (Figure 5) shows that the actual oxide thickness formed on carbon steel is much higher than the thickness attained from Eq. 10, and from the comparison of the actual pressures and the calculated pressure (Figure 6). The initial decline of the actual pressure is faster than that of the calculated one. This might be because the oxygen concentration inside the cavity used in the calculation ($C_{O_2}(x)$) is different from the actual O_2 concentration. The possible reasons for these are; 1) some changes in oxygen concentration occurred within the cavity at the initial step and during the exposure, 2) some oxides formed are Fe_3O_4 (from the assumption, all oxides are Fe_2O_3), and 3) the diffusivity of oxygen on the B-side may not be the same as the diffusivity of oxygen on the A-side because of the difference oxygen concentration (different driving force). In addition, the initial actual pressures were found to be lower than the calculated pressure suggesting that there might be leaking, as the test section was heated from room temperature to 400 °C which takes about 45 min. It is possible that some O_2 in the system were consumed in oxidizing the steel before the temperature reached 400 °C.

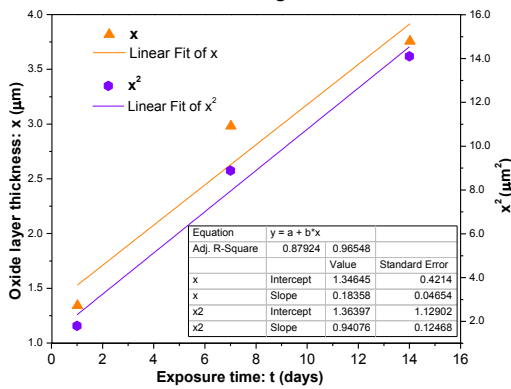


Figure 4: Relation between x or x^2 and exposure time for B-side of the 400 °C exposure samples.

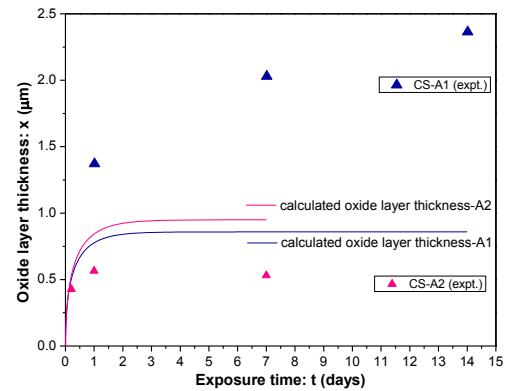


Figure 5: The plot of oxide layer thickness versus exposure time of carbon steel (A-side).

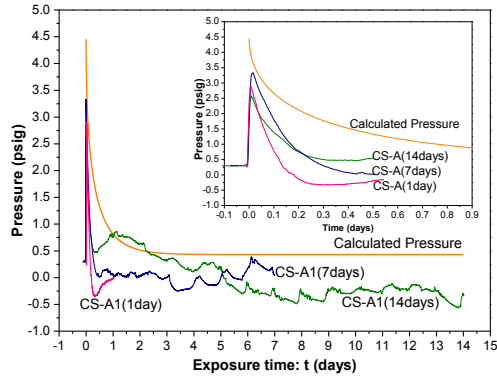


Figure 6: Relations between pressure inside the cavity and exposure time of the set 1 experiment.

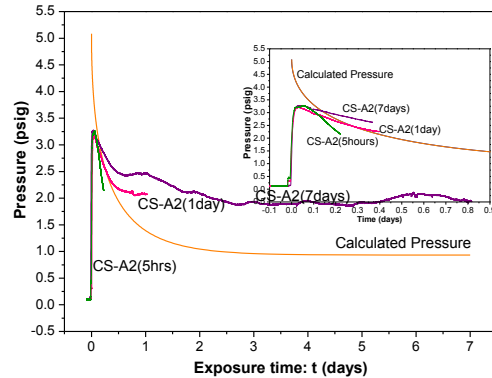


Figure 7: Relations between pressure inside the cavity and exposure time of the set 2 experiment.

Table 2: Data used in the calculation for Eqs. 10 and 13

Parameter	Value	unit	Parameter	Value	unit	Parameter	Value	unit
$MW_{Fe_2O_3}$	159.69	g/mol	$MW_{Fe_3O_4}$	231.533	g/mol	V_C	1.3×10^{-5}	m^3
$\rho_{Fe_2O_3}$	5.242×10^6	g/m^3	$\rho_{Fe_3O_4}$	5.17×10^6	g/m^3	A	26.42×10^{-4}	m^2
$C_{O_2,at 400^\circ C}$	3.80	mol/m^3	$C_{O_2,0}$	8.59	mol/m^3			

In experimental set 2 (A-side-2), assuming all oxides formed are Fe_3O_4 , the concentration of oxygen inside the cavity based on oxygen reacted to form the boundary layer becomes

$$C_{O_2}(x) = C_{O_2,0} - 2 \frac{\rho_{Fe_3O_4} Ax}{MW_{Fe_3O_4} V_C} \quad (11)$$

Applying Eq. 11 into the diffusivity equation, yields

$$\frac{x}{\left(1 - 2 \frac{\rho_{Fe_3O_4} Ax}{MW_{Fe_3O_4} V_C C_{O_2,0}}\right)} dx = \frac{1}{2} \frac{D_{O_2} MW_{Fe_3O_4} C_{O_2,0}}{\rho_{Fe_3O_4}} dt \quad (12)$$

Integrating Eq. 12 becomes

$$x - \frac{b}{a} \ln(ax + b) = act; \text{ where } a = -2 \frac{\rho_{Fe_3O_4} A}{MW_{Fe_3O_4} V_C C_{O_2,0}}, b = +1.0, \text{ and } c = \frac{1}{2} \frac{D_{O_2} MW_{Fe_3O_4} C_{O_2,0}}{\rho_{Fe_3O_4}} \quad (13)$$

As observed in Figure 5, the actual oxide thickness is lower than that obtained from Eq. 13 at a given exposure time. Figure 7 shows the discrepancy in pressure inside the cavity between the actual and calculated pressures of the experimental set 2. When compared with those of the experimental set 1, the actual pressures declined less. This might be due to the application of sealants. Therefore, if it was leaking, it should be at the beginning of the exposure.

4. Conclusions

The kinetics of oxide formation of carbon steel ASTM A-106B at 400 °C in atmospheric air (no change in O₂ concentration) was studied. The result showed that Hematite (Fe₂O₃) was formed in all cases and the reaction was controlled by diffusion of oxygen through the oxide layer. The diffusivity of oxygen through the oxide layer, $D_{O_2} = 7.05545 \times 10^{-14} \text{ m}^2/\text{s}$ and the parabolic rate, $k_p = 1.089 \times 10^{-17} \text{ m}^2/\text{s}$ were determined.

For the case of oxide formation 400 °C in atmosphere with reducing O₂ concentration during the exposure, the kinetics of oxide formation is also controlled by the diffusion of oxygen through the oxide layer. The experiments were separated into two sets; for the first set of experiments, the oxide formed on the surfaces exposed for 1 day and 7 days was Hematite (Fe₂O₃). Magnetite (Fe₃O₄) was found on 14 d exposure. In the experimental set 2, the oxide formed are Magnetite (Fe₃O₄) for the exposure time of 5 h, 1 d and 7 d, however, some Hematite (Fe₂O₃) was found at the 5 h exposure. Oxidation of CS A106B was not observed for the 90 °C exposure.

Acknowledgements

This work was carried out at the Centre for Nuclear Energy Research (CNER) as part of a fundamental study of the hydrogen probe project. The authors are grateful to colleagues at the CNER and the Chemical Engineering Department, UNB, especially Prof. D. H. Lister, Dr. Lui Lihui for helpful discussion. The authors are also grateful to the Petroleum and Petrochemical College and The Center of Excellence on Petrochemical and Materials Technology for supporting this paper.

References

- Bruzzoni P., Carranza R. M., 1999. "A pressure modulation method to study surface effects in hydrogen permeation through iron base alloys." *Electrochimica Acta* 44(24): 4443-4452.
- Leelasangsai C., 2009. Measurement of the hydrogen diffusion through various steels with and without oxide films. M.Sc, Chulalongkorn University.
- Piggott M. R. , Siarkowski A. C., 1972. Hydrogen diffusion through oxide films on steel, *Journal of the Iron and Steel Institute*: 4.
- Pyun S.-I. , Oriani R. A., 1989. The permeation of hydrogen through the passivating films on iron and nickel. *Corrosion Science* 29(5): 485-496.
- Schomberg K., Grabke H.J., 1996. Hydrogen permeation through oxide and passive films on iron. Duesseldorf, Stahleisen, Germany.